



**UNIVERSIDADE ESTADUAL DE CAMPINAS
SISTEMA DE BIBLIOTECAS DA UNICAMP
REPOSITÓRIO DA PRODUÇÃO CIENTÍFICA E INTELLECTUAL DA UNICAMP**

Versão do arquivo anexado / Version of attached file:

Versão do Editor / Published Version

Mais informações no site da editora / Further information on publisher's website:

<https://journals.aps.org/prb/abstract/10.1103/PhysRevB.60.4711>

DOI: 10.1103/PhysRevB.60.4711

Direitos autorais / Publisher's copyright statement:

©1999 by American Physical Society. All rights reserved.

DIRETORIA DE TRATAMENTO DA INFORMAÇÃO

Cidade Universitária Zeferino Vaz Barão Geraldo

CEP 13083-970 – Campinas SP

Fone: (19) 3521-6493

<http://www.repositorio.unicamp.br>

Point defect interactions with extended defects in semiconductors

A. Antonelli

Instituto de Física Gleb Wataghin, Universidade Estadual de Campinas, CEP 13083-970, Campinas, São Paulo, Brazil

J. F. Justo and A. Fazzio

Instituto de Física da Universidade de São Paulo, CP 66318, CEP 05315-970, São Paulo—SP, Brazil

(Received 21 April 1999)

We performed a theoretical investigation of the interaction of point defects (vacancy and self-interstitials) with an intrinsic stacking fault in silicon using *ab initio* total-energy calculations. Defects at the fault and in the crystalline environment display a different behavior, which is evidenced by changes in formation energy and electronic structure. The formation energies for the vacancy and the [110]-split interstitial are lower at the intrinsic stacking fault than those in the crystal, indicating that in nonequilibrium conditions, intrinsic stacking faults can act, together with other extended defects, as a sink for point defects, and also that in equilibrium conditions, there can be a higher concentration of such defects at the fault than that in bulk silicon. [S0163-1829(99)03631-0]

Extended defects in semiconducting materials have been a major concern over the past few years due to their effects on mechanical and electronic properties of these materials.¹ Dislocations, for example, control the material plasticity; they also give rise to energy levels in the gap. While experimental work has focused on studying dislocation and grain boundary properties, theoretical work at the atomistic level has been limited by the computational cost involved. Theoretical work has recently focused on the core properties of dislocations in silicon using empirical^{2,3} and *ab initio* methods.^{4,5} The interaction of point defects with extended defects in silicon has been considered for the case of vacancies interacting with dislocations⁵ and that of self-interstitials interacting with {311} defects.⁶

While dislocations and grain boundaries in semiconductors have been extensively investigated, only recently stacking faults have received attention.^{7–10} This is mainly because stacking faults in semiconductors have low energy (0.005 eV/Å² in Si), which make difficult any experimental identification. However, they play an important role in dislocation motion¹¹ and, consequently, in plasticity. In a zinc-blende semiconductor, full dislocations belonging to the {111} glide planes dissociate into partial dislocations having a stacking fault (SF) connecting the partials.¹¹ This dissociation is energetically favorable and facilitates the dislocations to glide conservatively. Dislocation mobility is controlled by thermal kink processes,¹¹ but point defects can participate in these processes. Vacancies are known to migrate to dislocation cores, where defect diffusivity is orders of magnitude higher than in the crystalline environment. Recent theoretical work¹² has shown, at least for fcc metals, that the stacking fault ribbon also participates in the vacancy migration processes.

A stacking fault is an irregularity in the stacking sequence of the material. In zinc-blende materials, the normal stacking sequence in the [111] (close-packed) direction is ... AaBbCcAaBbCc... where each letter represents a stacking plane.¹¹ An intrinsic SF (ISF) is equivalent to removing a double layer (Bb, for example) and glueing to-

gether the remaining material. An extrinsic SF (ESF), on the other hand, is equivalent to adding a double layer. This work will focus only on the intrinsic stacking fault, since experimental findings have identified it as the prevailing stacking fault in silicon.¹³ The nearest neighborhood of an atom at the SF remains unaltered, when compared to that of an atom in the crystalline environment, preserving the original tetrahedral symmetry. However, this symmetry is changed as one considers second-nearest neighbors.⁹ In other words, starting from the second-nearest neighbors, the environment surrounding a point defect at a SF differs from that seen by the same defect in the perfect crystal. Therefore, some properties, such as the formation energy and the electronic structure, of a defect in a crystalline environment may change if the same defect is placed at a SF. This effect has already been discussed in the context of metals. Suzuki¹⁴ has pointed out that solute atoms segregate at stacking faults, by lowering the stacking fault energy with the increasing concentration of the solute atoms. Besides, oxygen segregation in silicon stacking faults has been reported.^{15,16}

In this paper we present a comparative study of electronic and structural properties of intrinsic point defects at an ISF and in a crystalline environment in silicon. The total-energy calculations were performed within the density-functional theory and the local-density approximation framework.¹⁷ Figure 1 shows the reference periodic supercell containing 120 atoms used in the calculations to simulate the isolated ISF, as well as the point defects. The orthorhombic supercell consists of five double-layers stacked along the [111] direction. The infinite intrinsic stacking fault perpendicular to the [111] direction is shown at the double-layer labeled: ISF in Fig. 1. Atoms at the double-layer labeled: CL in Fig. 1 are at a distance of 7.8 Å from the ISF and their surrounding environment is that of an atom in a perfect crystal up to the fourth-nearest neighbor. Thus, these atoms can be considered approximately as bulklike atoms. All the calculations we performed were done using the 120-atom supercell with an ISF as reference and placing the point defects at the ISF and in the bulklike site. Therefore, the defect properties at the ISF

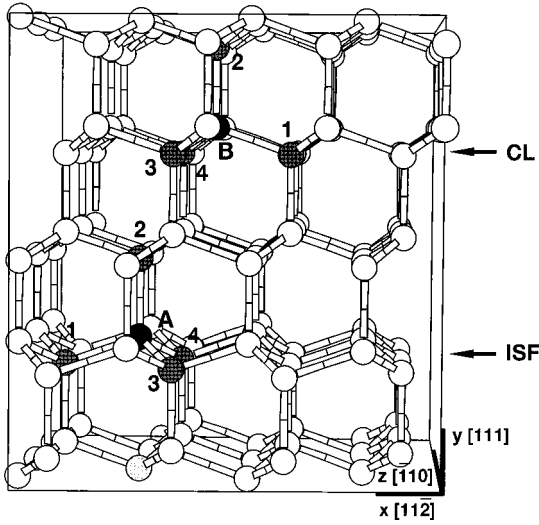


FIG. 1. Structure consisting of a 120-atom orthorhombic supercell used in the calculations. x , y , and z axes are, respectively, parallel to the $[11\bar{2}]$, $[111]$, and $[\bar{1}10]$ directions of the diamond cubic lattice. The cell has one ISF in the xz plane. Details in the text.

and in the crystalline environment are computed within the exact same approximations. This kind of approach has been used previously to determine the segregation energy of impurities to grain boundaries¹⁸ and dislocation cores¹⁹ in silicon. The Kohn-Sham equations were solved using the Car-Parrinello scheme²⁰ with pseudopotentials²¹ in the Kleinmann-Bylander form.²² The valence electrons wave functions were expanded in a plane-waves basis set, with kinetic energy up to 10 Ry. The sampling in the Brillouin zone was performed using the Γ point. Geometry optimization of the atomic structure was performed by moving the atoms until the Hellmann-Feynman forces were smaller than 0.001 Ry/a.u. The calculations were performed without imposing any symmetry constraints. In order to check the quality of our approximations we performed a calculation of the electronic structure of the system containing only the ISF. The valence-band width obtained is only 0.04 eV larger than the bandwidth of the projected valence of the perfect crystal. The projected bands of the perfect crystal were obtained using an orthorhombic 144-atom cell. From the calculations with the 120-atom supercell we found at the Γ point a doubly degenerate and fully occupied defect level at 0.1 eV above the top of the valence band. We also found a defect level 0.1 eV below the bottom of the conduction band. These findings are in good agreement with earlier calculations also using *ab initio* pseudopotentials.²³

We first analyze our results for the single vacancy. Figure 1 shows the first-nearest neighbors (dark gray atoms), labeled 1, 2, 3, and 4, of an atom at the ISF and in the crystal (black atoms). In the perfect crystal, a silicon atom has four first-nearest neighbors at 2.35 Å and 12 second-nearest neighbors at 3.84 Å. Aside from these neighbors, a silicon atom at an ISF has an extra neighbor at a distance of 3.91 Å (light-gray atom in Fig. 1), which is very close to the second-nearest neighbor distance.⁹ The total-energy calculations indicate that at the ISF the vacancy has its formation energy lowered by 0.23 eV with respect to that of the bulklike site,

TABLE I. Distances between the four atoms first-nearest neighbors of the vacancy (labeled 1, 2, 3, and 4 as in Fig. 1) at the ISF and in a crystal-like site (CL) (in Å).

	1-2	1-3	1-4	2-3	2-4	3-4
ISF	2.75	3.31	3.29	3.45	3.44	3.47
CL	2.78	3.41	3.39	3.45	3.43	3.42

which suggests a significant effect arising from the changes in the second-nearest neighbors. The distances between the first nearest neighbors of the vacancy are given in Table I. In both cases, for the vacancy at the ISF and in the crystal, there is an inward relaxation of these atoms, since the distance between these atoms in the perfect crystal is of 3.84 Å. Aside from an inward relaxation, a Jahn-Teller distortion takes place, breaking up the local tetrahedral symmetry, lowering it to a local C_{2v} symmetry. This distortion corresponds to one of the T_2 modes of distortion of the vacancy.²⁴ The C_{2v} symmetry, instead of the usual D_{2d} , is likely caused by the lowering of the symmetry of the system due to the presence of the ISF. We also notice a small breaking of the C_{2v} symmetry for the vacancy at the ISF. In this case, the distances between atom 1 to atoms 3 and 4 are slightly smaller than those between atom 2 to atoms 3 and 4 (see Table I). This symmetry breaking is possibly caused by the additional second-nearest neighbor to the vacancy at the ISF, which is closer to atom 1 than to atom 2.

We now discuss the results of the study on self-interstitials. The $[110]$ -split interstitial (I_S) in Si is regarded to be the self-interstitial with the lowest formation energy.²⁵ In this case, the lattice site is empty and two atoms form a dumbbell aligned along the $[110]$ direction. For the $[110]$ -split interstitial, the environment outside and at the fault are considerably different. Figure 2(a) shows a side view of the split interstitial (black atom) in a crystal-like environment, whereas Fig. 2(b) depicts the defect at the ISF. The plane of the figure is perpendicular to the $[110]$ direction and only one of the atoms of the dumbbell is visible. We chose this perspective to show the differences in the local crystalline structure surrounding the split interstitial in both environments (gray rings). Our results indicate that the formation energy of the I_S at the ISF decreases by 0.61 eV with respect to that in a crystal-like site. This large difference in the formation energy can be explained by the local structure close to the fault. Although the planar packing is identical in the crystal and at the stacking fault, the local structure around the defect at the ISF allows for a larger relaxation than that in the crystal-like environment. For instance, it can be seen in Fig. 2 that there are atoms closer to the defect (black atom) in the crystal-like site than when it is at the ISF, due to differences in the sixfold rings of atoms (gray rings) in each one of the situations. In Fig. 3(a) we show the total charge density on a $\{110\}$ plane, which contains the split interstitial in a crystallike environment in the middle lower chain of atoms. This plane is shown as a dashed line in Fig. 2(a). In this case, the atoms in the dumbbell are 2.48 Å apart with a weak bond between them, which is in reasonable agreement with recent calculations in the literature.²⁶ Figure 3(b) displays the total charge density on the equivalent plane in the case that the split interstitial is at the ISF. One can still see

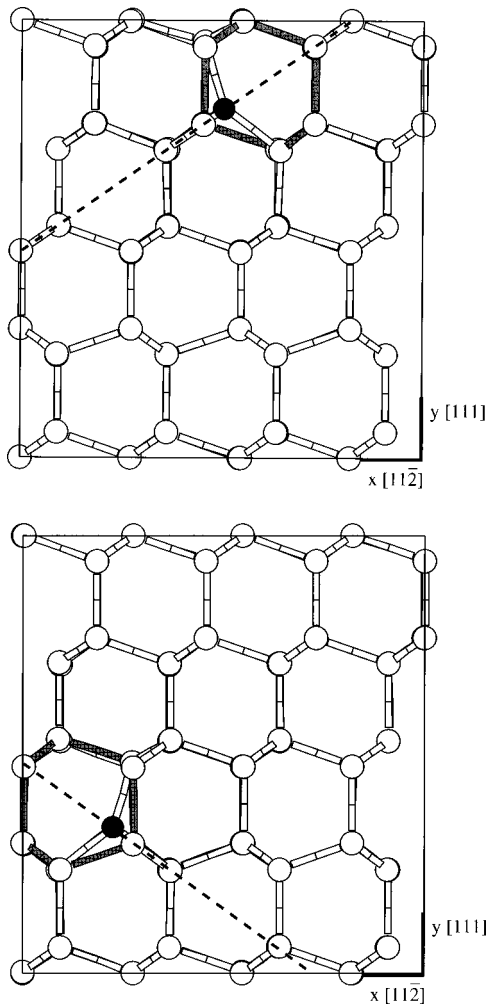


FIG. 2. Structure of a $[110]$ -split interstitial (a) in a crystal-like environment (top) and (b) at the ISF (bottom). Details in the text.

the split interstitial in a lower chain of atoms, but there is no equivalent chain in the upper part of the picture, in fact it shows a completely different environment. The reason for that is clear from Fig. 2(b) where the plane we are considering now is shown by the dashed line. In this case, instead of containing another zigzag chain of atoms the plane contains a linear chain of atoms, which can be seen in the upper part of Fig. 3(b). One can also see that the bond between the atoms in the dumbbell is weaker than that of the interstitial in the crystal-like site. The charge density around the defect is more delocalized. The distance between the atoms in the dumbbell for the split interstitial at the ISF is 2.52 \AA , which indicates larger relaxations of the system, resulting in lower formation energy.

We now compare the interstitial in an hexagonal site (I_H) in the crystal and at the ISF. The difference in total energy between these two cases is 0.15 eV , which is smaller than those obtained for the other defects we have considered. The six-atom ring of first-nearest neighbors of the interstitial atom is equivalent in both cases. In the crystalline environment, the interstitial atom has eight second-nearest neighbors, at a distance of 3.50 \AA . For the case of the I_H at the ISF the number of second-nearest neighbors is reduced to six. That explains the lowering in the formation energy of the defect at the fault. However, our results indicate that, in this

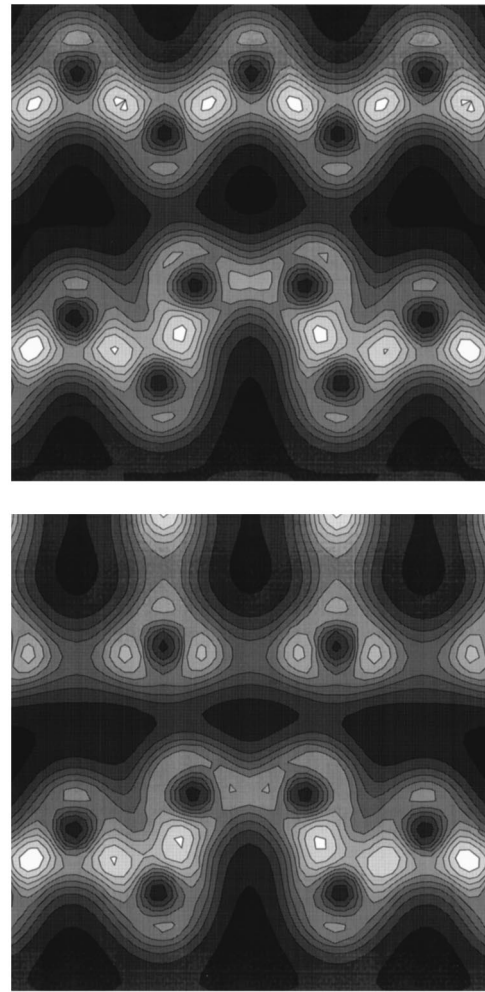


FIG. 3. Total charge density on a $\{110\}$ plane that contains a $[110]$ -split interstitial (a) in a crystal-like environment (top) and (b) at the ISF (bottom). Details in the text.

case, the second-nearest neighbors do not play a very important role. Another important interstitial structure in Si is the tetrahedral one (I_T), which is located at a distance of half bond length (1.18 \AA) along the $[111]$ direction from the hexagonal interstitial site. In the crystal, a I_T has four first-nearest neighbors. However, there is no such site at the ISF. Due to the fault in the stacking sequence, the equivalent site (half a bond length away from the I_H) has only three first-nearest neighbors. The missing nearest neighbor would render the site unstable and the interstitial would relax down to the closest hexagonal site at the ISF.

In conclusion, we have investigated the effects of a stacking fault on the properties of intrinsic point defects in silicon. In equilibrium conditions, there would be a higher concentration of defects at the fault as result of lower formation energy. The difference in formation energy suggests that in nonequilibrium conditions, such as after irradiation, the fault could act as a sink for point defects. In highly irradiated materials the stacking faults, formed under deformation as result of dislocation splitting and motion, should not be as clean as generally thought. Instead, the faults would have substantial concentration of defects. This could affect dislocation mobility. Recent theoretical calculations found binding energies up to 2.0 eV for a vacancy inside the core of a

partial dislocation in silicon⁵ and that self-interstitials are attracted to $\{311\}$ defects.⁶ This is consistent with our finding of lower formation energies at the fault. Since partial dislocations are at the edge of a stacking fault, defects, which eventually migrate towards the dislocation cores, may first migrate to the stacking faults. Therefore, the stacking fault would play an important role in pipe diffusion of point defects through dislocations.¹²

Results of several experiments on the electrical activity of dislocation related defects in semiconductors have been reviewed recently.^{1,27} Deformation induces several active centers, which have been associated to specific structures related to vacancies in the dislocation cores.²⁷ In the light of our results, this picture is considerably more complex because vacancy centers at the stacking fault may also be electrically

active and provide additional peaks in the spectra related to active centers.

We also speculate that a stacking fault can be an efficient tool to investigate the effect of second- (and higher-order) nearest neighbors on a point defect, since an atom at the SF has the same first-nearest neighbors as one in a crystalline environment.⁹ Therefore, the larger the difference in structure and formation energy for a defect at and far from the SF, the larger the interaction of high-order neighbors with this defect.

The authors acknowledge partial support from the Brazilian funding agencies FAPESP and CNPq. Computer calculations were performed at the facilities of CENAPAD-SP.

-
- ¹H. Alexander, in *Dislocation in Solids*, edited by F. R. N. Nabarro (North-Holland, Amsterdam, 1986), Vol. 7, p. 115.
- ²V.V. Bulatov, S. Yip, and A.S. Argon, *Philos. Mag. A* **72**, 453 (1995).
- ³V.V. Bulatov, J.F. Justo, W. Cai, and S. Yip, *Phys. Rev. Lett.* **79**, 5042 (1997).
- ⁴G. Csányi, S. Ismail-Beigi, and T.A. Arias, *Phys. Rev. Lett.* **80**, 3984 (1998).
- ⁵N. Lehto and S. Öberg, *Phys. Rev. B* **56**, 12 706 (1997).
- ⁶J. Kim, J.W. Wilkins, F.S. Khan, and A. Canning, *Phys. Rev. B* **55**, 16 186 (1997).
- ⁷P. Käckell, J. Furthmüller, and F. Bechstedt, *Phys. Rev. B* **58**, 1326 (1998).
- ⁸C. Stampfl and C.G. Van de Walle, *Phys. Rev. B* **57**, 15 052 (1998).
- ⁹L.F. Mattheiss and J.R. Patel, *Phys. Rev. B* **23**, 5384 (1981).
- ¹⁰N. Lehto, *Phys. Rev. B* **55**, 15 601 (1997).
- ¹¹J. P. Hirth and J. Lothe, *Theory of Dislocations* (Wiley, New York, 1982).
- ¹²J. Huang, M. Meyer, and V. Pontikis, *Phys. Rev. Lett.* **63**, 628 (1989).
- ¹³K. Wessel and H. Alexander, *Philos. Mag.* **35**, 1523 (1977).
- ¹⁴H. Suzuki, *J. Phys. Soc. Jpn.* **17**, 322 (1962).
- ¹⁵S.M. Hu, *J. Appl. Phys.* **45**, 1567 (1974).
- ¹⁶S. Senkader, J. Esfandiyari, and G. Hobler, *J. Appl. Phys.* **78**, 6469 (1995).
- ¹⁷P. Hohenberg and W. Kohn, *Phys. Rev.* **136**, 864B (1964); W. Kohn and L.J. Sham, *ibid.* **140**, 1133A (1965).
- ¹⁸A. Maiti, M.F. Chisholm, S.J. Pennycook, and S.T. Pantelides, *Phys. Rev. Lett.* **77**, 1306 (1996).
- ¹⁹T. Kaplan, M. Mostoller, and M.F. Chisholm, *Phys. Rev. B* **58**, 12 865 (1998).
- ²⁰R. Car and M. Parrinello, *Phys. Rev. Lett.* **55**, 2471 (1985).
- ²¹G.B. Bachelet, D.R. Hamann, and M. Schluter, *Phys. Rev. B* **26**, 4199 (1982).
- ²²L. Kleinman and D.M. Bylander, *Phys. Rev. Lett.* **48**, 1425 (1982).
- ²³M.Y. Chou, M.L. Cohen, and S.G. Louie, *Phys. Rev. B* **32**, 7979 (1985).
- ²⁴J. Bourgoin and M. Lannoo, *Point Defects in Semiconductors II* (Springer, Berlin, 1983), Vol. 35.
- ²⁵P.E. Blöchl, E. Smargiassi, R. Car, D.B. Laks, W. Andreoni, and S.T. Pantelides, *Phys. Rev. Lett.* **70**, 2435 (1993).
- ²⁶J. Zhu, T. Diaz de la Rubia, L.H. Yang, C. Mailhot, and G.H. Gilmer, *Phys. Rev. B* **54**, 4741 (1996).
- ²⁷J. Weber, *Solid State Phenom.* **37-38**, 13 (1994).